A CONTRIBUTION TO THE MATERIAL TEXTURE ANALYSIS FROM X-RAY DIFFRACTION DATA

Erika HUJOVÁ* – Vladimír ÁČ

Faculty of Special Technology, Alexander Dubček University of Trenčín, Pri parku 19, 911 06 Trenčín, Slovakia
**Corresponding author E-mail address: erika.hujova@tnuni.sk*

Abstract

The paper deals with possibilities of texture analysis of metal alloys using X-ray diffraction. The basic principles of the methodology, experimental equipments and procedures are shown. There are described a measuring methods of pole patterns and orientation distribution function of texture and interpretation of the results for practical use. Finally, we will show some of the results of measurements on α-brass CuZn30.

Keywords: X-ray diffraction, polycrystalline materials, pole figures, ODF – orientation distribution function, texture analysis, α-brass CuZn30

1 Introduction

Polycrystalline materials have been frequent object of research and today it is no different. Unlike the past, metallographic methods have been developed further thanks to the possibilities that entail development of computer technology. These include a texture analysis of polycrystalline materials.

Techniques using X-ray diffraction is very old [1] and in texture analysis has an irreplaceable role. In a sense, it is complementary to the methods, consisting of the diffraction of photons. While electron microscopy allows study of the structural details at the nanometric scale, X-ray diffraction provides a parameter, which is averaged over a relatively large sample volume. Electron microscopy has excellent resolution in real space, on the other hand x-ray diffraction in angular space.

In recent decades thin films have become an inevitable and important part of the materials research and modern technologies. Each property of a thin film is more or less depends on their structure. A prerequisite of any technological progress in this area is therefore detailed information on the structural parameters of thin films [2,3].

Knowledge of the structure and texture of polycrystalline materials is necessary because both are the result of the technological process and at the same time determine the characteristics of the material. The very notion of texture characterizes and describes the preferential orientation of the crystallites of the polycrystalline material. Anisotropy of the resulting material is then given by anisotropy grains themselves and also their orientation [4].

Like other counting technique, the analysis of texture undergone certain methodological developments. First, the texture geologists pay for the study of geological processes and transformations of rocks and minerals Earth's surface. With the advent of industrial production and development of new materials, there is still paid careful attention to texture [5]. First, describing the texture by measured pole figures, later, with the advent of computer technology, the texture is described by the orientation distribution function (ODF) [6].

2 X-Ray diffraction and texture analysis

2.1 X-ray diffraction

X-ray radiation used in texture analysis is the electromagnetic radiation of wavelength λ from 0.01nm to 5 nm. X-ray spectrum emitted by the copper anode of the X-ray tube consists of two components, the continuous and characteristic spectrum. The continuous part of the spectrum is known as the white radiation. It arises by braking incident electrons in an electric field of nuclei or by ionization of atoms.

The characteristic electron radiation originates from one stamping of internal energy levels of atoms and the subsequent transfer of electrons from higher levels on the loose surface. The wavelength of the emitted radiation energy determines the difference appropriate levels of atoms. Characteristic spectra are classified according to levels, from which the electron has been discarded, as the series K, L, M, ... (Fig. 1, Fig. 2).

The wavelengths of the three strongest lines of the characteristic spectrum of a copper anode of the X-ray tube, which is used most often, are shown in the Table 1.

Table 1 *The wavelength of lines in the characteristic spectrum for copper anode of the X-ray tube[7]*

Line	$\mathbf{K_{\alpha 1}}$	$\mathbf{K_{\alpha 2}}$	$\mathbf{K_{\beta}}$
λ[nm]	0,154056	0,154439	1,39217

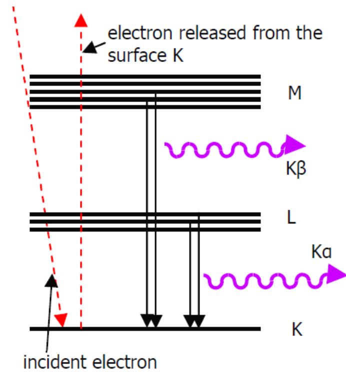

Fig. 1 *Energy levels of the atom and transitions of electrons [7]*

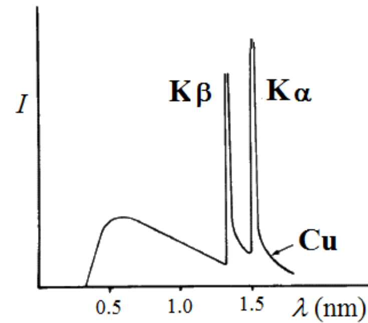

Fig. 2 *Cu anode X-ray spectrum*

Upon impact of the X-ray on crystalline substance, there is scattering of radiation on scattering centers, (the individual atoms making up the crystals). Since atoms are periodically three-dimensionally arranged in crystals, under certain conditions, may the interference of coherent scattered waves arise and intense diffracted bundle may be registered in some directions in space.

Geometrical conditions of diffraction in the case of three-dimensional periodic structures down Laue diffraction conditions. Conditions of diffraction can also be determined by Bragg's law (1), which is based on the concept of the planes of the crystal lattice (Fig. 3). A set of mutually parallel lattice planes are described by triplet of Miller indices (hkl) and characterized by distance d_{hkl}.

$$2d_{hkl} \sin \Theta = n.\lambda \,, \qquad (1)$$

where n is an integer (1,2,…). Bragg's law expresses known condition for the creation of interference in the optics - track difference of the two beams is an integer multiple of the wavelength λ. If reflected X-rays beams are in phase, they occur reinforcement of the beam or constructive interference.

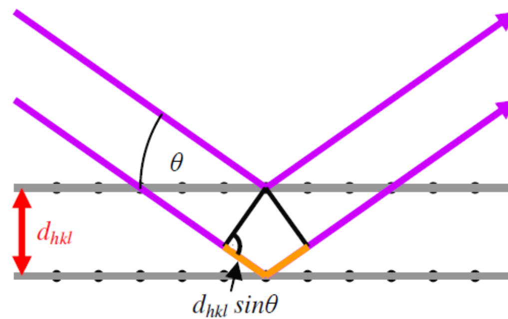

Fig. 3 *Bragg's law*

The angle of incidence θ measured by diffracting {hkl} planes (the condition of interference) is called the Bragg's angle. The distance d_{hkl} between two lattice planes is given by (2). In this equation a is a lattice constant.

$$d_{hkl} = \frac{a}{\sqrt{h^2 + k^2 + l^2}} \qquad (2)$$

2.2 Analysis of polycrystalline layers

Polycrystalline material consists of a vast number of grains - crystallites that are randomly oriented in space. Upon impact the X-ray on the sample, the Bragg's condition of diffraction is fulfilled for a sufficient number of crystallites even when the sample is stationary. In various crystallites diffraction occurs on different systems of crystal planes that are characterized by interplanar distance d_{hkl}. Although the whole spectrum of X-ray lamp incident on the sample (the simplest experimental setup), detectable diffraction originate only for the most intense lines of characteristic spectrum, i.e. doublet $K_{\alpha 1,2}$ and K_{β}.

Since the diffraction from K_β line does not bring any new information about the sample, on the contrary make diffraction report less transparent, K_β line of the X-ray spectrum is removed by β-filter now at X-ray radiation output of the lamp.

By Bragg's law, between diffracted beams from different planes (hkl) and incident beam there are different angles $2\theta_{hkl}$ (Fig. 4). The basic technique of registration of radiation diffracted on the sample is so called θ/2θ measurement. Equipment operating in this mode is called θ/2θ diffractometer. Outcome measurements are presented as a graph of intensity depending on the angle 2θ.

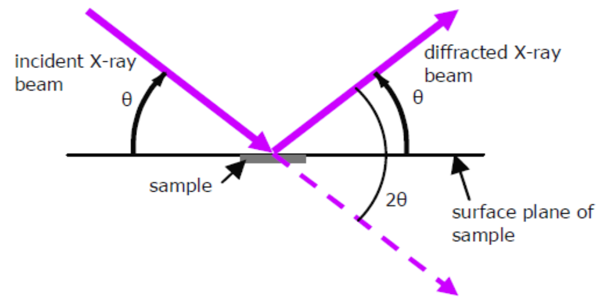

***Fig. 4** Principle of θ/2θ measurement [7]*

In the case X-ray diffraction on polycrystalline materials, only grains with diffraction planes parallel to the surface of the sample contribute to the diffracted beam registered by detector (Fig. 5). Different groups of grains contribute to different diffraction with different Bragg's angles.

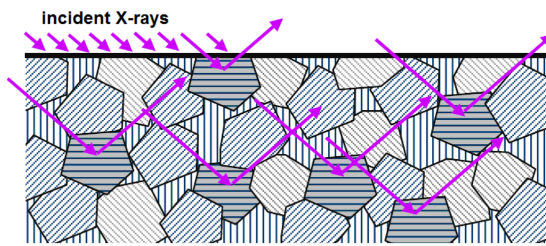

***Fig. 5** X-ray diffraction on group of grains of polycrystalline materials[7]*

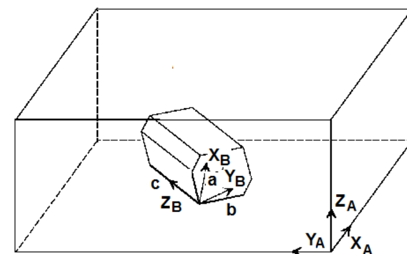

***Fig. 6** Crystal and sample coordinate system*

2.3 Texture and anisotropy of crystalline materials

A crystal is characterized by the periodic arrangement of its elements (atoms, ions) in space. This always generates a dependence of the crystal properties on the chosen direction, which is called anisotropy.

Most natural or artificial solids (rocks, ceramics, metal alloys or polymers) contain of many crystallites of different size, shape and different orientations. They are usually multi-phase substances, i.e. they contain several crystalline phases of different structure. The most important parameter describing the anisotropy of polycrystalline materials is their texture. Via the anisotropy of physical properties due to the lattice structure, a regular texture in which the crystallites of one phase have only a few preferred orientations produces anisotropy of the polycrystalline material as well.

The great variety of texture-modifying processes described an even greater number of material-specific textures, since the different phases present in a material react differently due to their structure and properties; this is also documented by different textures. Therefore, the knowledge of the initial and final textures of a sample is the most important precondition for the investigation and description of texture-modifying processes and their conditions. Only this knowledge allows the systematic manipulation of anisotropic properties in polycrystalline materials (manufacture of design materials).

2.4 Crystal and sample coordinate systems

To describe the orientations of a crystallite, Cartesian right-hand coordinate systems must be fixed for both the sample and the crystallite. Uniform conventions must be agreed for the application of the coordinate systems to allow the comparability of various textures.

The sample coordinate system K_A is usually adapted to the process geometry if it is known. Thus, the rolling direction R is selected parallel to X_A and the normal direction N is selected parallel to Z_A for a rolled sample (Fig. 6). The crystal coordinate system K_B should be fixed to the basis vectors a, b and c of the Bravais lattice as follows:

$$Z_B \parallel c,\ Y_B \parallel c \times a,\ X_B \parallel Y_B \times Z_B. \tag{3}$$

Crystal and sample symmetry are the reason that there are several equivalent possibilities for fixing the crystal and sample coordinate system. Evidently the crystal symmetry does not lead to a multiplication of the crystallite orientation since the crystal lattice is projected on itself by the symmetry operations. In contrast, the sample symmetry produces the existence of several crystallites with evidently different orientations which are, however, equivalent in terms of the sample symmetry.

2.5 Texture measurement

Texture measurement is based on the registration of intensity of the selected diffraction for different rotation of the sample at a detector's fixed position. The intensity of the radiation is proportional to the number of crystallites, which are for a given orientation of the sample in a diffraction position.

Crystallite orientation in polycrystalline thin films is rarely isotropic. Mostly preferential orientation of some crystallographic direction is observed - usually with a low direction index. This direction relates to the orientation of underlay and they used to be perpendicular to themselves (Fig. 7). A thin layer has a preferential orientation - texture.

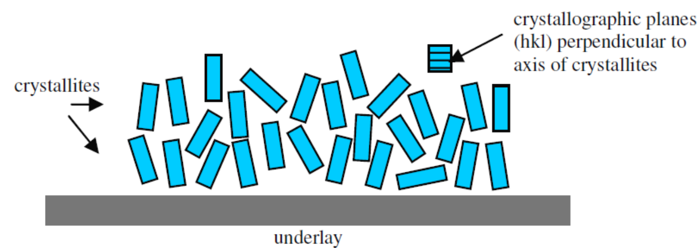

Fig. 7 *Schematic structure layout [7]*

A special sample holder is required to achieve full texture analysis by X-ray diffraction, called texture goniometer. It enables a rotation about an axis perpendicular to the plane of the sample - φ axis and turning aside of the sample about a horizontal - axis χ (Fig. 8).

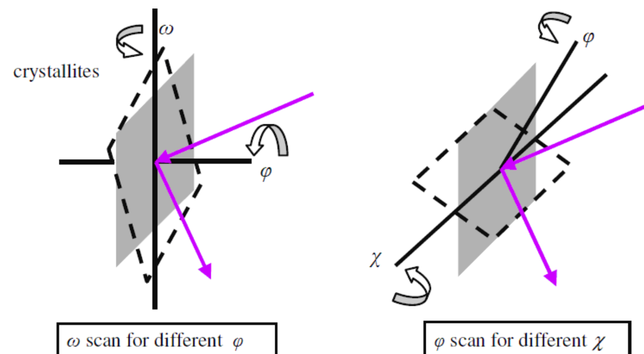

Fig. 8 *Two ways to texture measurement [7]*

From the beginning, the texture of polycrystalline materials, especially metal, was determined by X-ray diffraction on specially designed texture goniometer. Textural goniometers are becoming increasingly sophisticated, their operation is computer controlled and programmed to evaluate the texture and the resulting anisotropic properties of materials is a series of program files that are processed measured data. Still it is necessary to know the basic principles and theoretical knowledge in evaluating textures. It is necessary to understand the concepts such as symmetry, coordinate system, the orientation, ideal orientation of crystallites, Euler angles [3], stereographic projection, projection standard single crystal structure of pole figures, ODF. Calculated values of the coefficients of normal anisotropy are interesting for the practice.

Conventional $\theta/2\theta$ diffractometers allow partial texture analysis using the so-called ω-curves (Fig. 9) in a fixed position of the detector and rotation the sample only around the basic - ω axis of diffractometer . The range of these measurements is limited by the size of the Bragg's diffraction angle. Therefore the texture analysis can not be complete. However, the ω-curves can be measured for different rotation around sample's normal. In the absence of φ axis this rotation can be done manually.

A thin film is formed by crystallites of rectangular shape. The crystallites are oriented so that their long axis is rotated in a direction approximately perpendicular to the underlay. A ω-curve of diffraction planes (hkl) reaches a maximum when the angle ω is equal to the Bragg's angle θ.

To describe a measurement of the width of an object in a picture, when that object does not have sharp edges, the method of full width of the image at half maximum value is used. Full-width half-maximum (FWHM) is a simple and well-defined number (Fig.10) which can be used to compare the quality of physical effects under different observing conditions. FWHM of the curves tells about a certain texture in the sample. FWHM corresponds to a degree of directional arrangement.

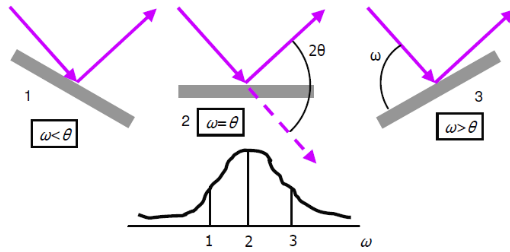

Fig. 9 *Model of the ω - curve [7]*

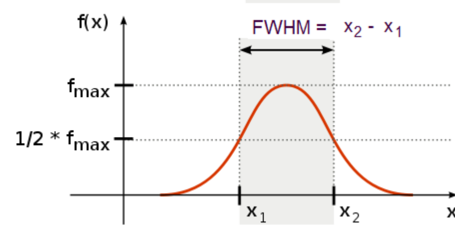

Fig. 10 *An explanation of FWHM (full width at half maximum)*

Accompanying phenomenon of every technological process (mechanical, thermal or chemical) is the formation of mechanical stresses in materials. These usually remain in the material after the completion of the process, so they are often referred as residual stresses. Tensions are generally non-homogeneous, and may vary significantly in various sizes ranging from a diameter comparable to the interatomic distances to several tens of nm dimensions. The macroscopic stress is tension approximately homogeneous in a macroscopic area of the material. The polycrystalline material is represented by a systematic shift of diffraction maxima, which allows their measurement using X-ray diffraction. Due to the strong absorption of X-ray diffraction it allows to analyze the mechanical stress only near-surface layer of material with a thickness of several microns.

2.6 Pole figures

Texture is often represented using a pole figure, in which a specified crystallographic axis (or pole) from each of a representative number of crystallites is plotted in a stereographic projection, along with directions relevant to the material's processing history. These directions define the so-called sample reference frame because the investigation of textures started from the cold working of metals. These directions are usually referred as the rolling direction, the transverse direction and the normal direction. For drawn metal wires the cylindrical fiber axis turned out as the sample direction around which preferred orientation is typically observed.

View of texture is very specific task. The results of full texture measurements are presented in the form of so-called pole figures (Fig.11). Pole figures provide the first picture of the texture sample, without quantitative evaluation. The distribution function of orientation of crystallites is defined on the reference sphere area - pole figure is a special part of projection of this area to the plane (Fig.12). The center of pole figure corresponds to the normal of the sample surface.

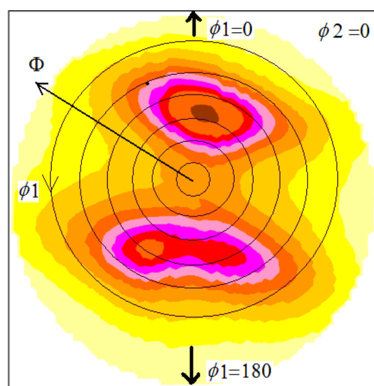

Fig. 11 *An example of pole figure*

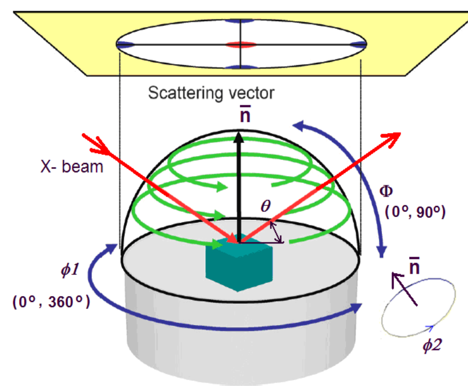

Fig. 12 *Sphere of fixed-length scattering vector and stereographic projection [3]*

2.7 Orientation distribution function (ODF)

The full 3D representation of crystallographic texture is given by the orientation distribution function (ODF) which can be achieved through evaluation of a set of pole figures or diffraction spectra. Subsequently, all pole figures can be derived from the ODF [3].

The ODF is defined as the volume fraction V of grains with a certain orientation g:

$$ODF(g) = \frac{1}{V}\frac{dV(g)}{dg} \tag{4}$$

The space g is identified using three Euler angles (ϕ_1, Φ, ϕ_2). The Euler angles (see Fig. 12) then describe the transition from the sample's reference frame into the crystallographic reference frame of each individual grain of the polycrystalline. One thus ends up with a large set of different Euler angles, the distribution of which is described by the ODF. ODF is normally displayed as a set of rusts of Euler space for one of its constant angle to comprehensively characterize the texture of the sample. A relatively large number of inter-related cuts, however, can " fog " some important facts.

The orientation distribution function, ODF, cannot be measured directly by any technique. Traditionally both X-ray diffraction and EBSD may collect pole figures. Different methodologies exist to obtain the ODF from the pole figures or data in general. They can be classified based on how they represent the ODF. Some represent the ODF as a function, sum of functions or expand it in a series of harmonic functions. Others, known as discrete methods, divide the ODF space in cells and focus on determining the value of the ODF in each cell [3].

3 Experimental results

In our experiment, we examined samples of α-brass CuZn30 with chemical composition according to DIN17660.W, No. 2.0256. The microscopic surface structure is shown in Fig.13. Four samples with different rolling rate ε (*Table 2*) were used. The measurements were made in Institute of Electrical Engineering of Slovak Academy of Sciences in Bratislava on Bruker diffractometer with Cu rotation anode.

***Table 2** Samples of deep drawn brass CuZn30 (Cu – 70%, Zn – 30%)*

Sample indication	Rolling rate ε
S0	annealed without deformation
S3	cold rolled – ε = 22,0%
S4	cold rolled – ε = 35,0%
S6	cold rolled – ε = 53,3%

In first step, the basic diffraction response was measured. Result is shown in Fig.14. There is possible to see the lines from copper face-centered cubic (FCC) structure plane (111) and (200).

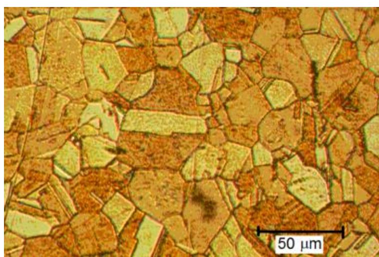

Fig. 13 The texture of CuZn30
Cu – cubic (FCC), Zn – hexagonal (HCP)

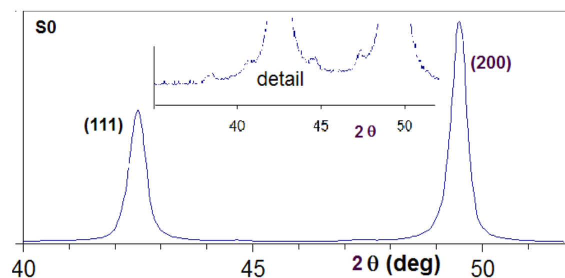

***Fig.14** Basic diffraction response*

The small picks are associated to other planes (lattice constant of Cu is a = 0,36146 nm and atom radius R = 0,128 nm, $\sqrt{2}\,a = 4R$) [8]. Zn crystallize in hexagonal close-packed (HCP) lattice (a = 0,2665 nm, c = 0,4947 nm, R = 0,133 nm). In alloys the lattice constant is also changed due to arrangement of individual atoms in the crystal lattice. The pole figures were measured for planes (111), (200) and (220).

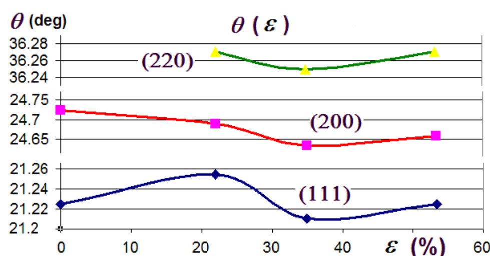

***Fig.15** Variations of θ angle for various crystal diffraction planes in dependence on deformation level*

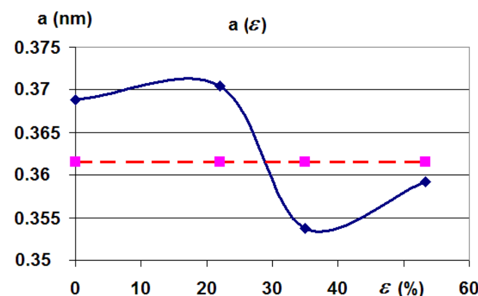

***Fig.16** Deviation of lattice constant S0 in dependence on deformation level dashed line –declared value [6]]*

There were the small variations in incident diffraction angle θ indicated (see Fig. 15) in dependence of ε (sample thickness reduction) [9]. This is a result of residual stresses in the material after mechanical deformation [10]. Real deviation of lattice constant is seen from Fig.16. The shape of this dependence indicates a complicated arrangement process of the material grains at mechanical deformations. The pole figures for crystalline plane (111) of all four brass samples are shown in Fig. 17. The pole figure from crystalline planes (200) and (220) for these analyses were not used. The pole figures data (Fig.17) show that change of the position and intensity of the diffraction response comes with increasing deformation. This is natural [11], because the orderliness of crystalline grains increased at deformation, in terms of the orientation of the crystalline planes.

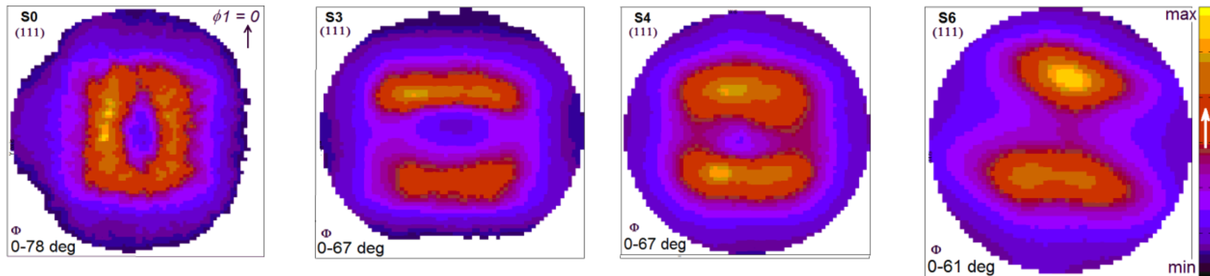

Fig.17. Pole figures of mechanically deformed brass (CuZn30) strips for plane (111)

Some of these results were published in [12]. The orientation distribution function of crystalline planes from pole figure can be displayed in orthogonal form. The ODF constructed from pole figures are presented in Fig. 18. These curves for all measured angles of samples inclination Φ show the plane distribution for various rotation angle ϕ_1 at $\phi_2 = 0$ deg. These curves also obtain information about the preferred directions of crystallographic planes caused by mechanical deformation. The angle between the plane (111) and the walls of the crystal is $\phi = 54{,}735$ deg. Complementary angle to 90 deg ($\phi' = 35{,}265$ deg) will be one of the tilt incident angles for crystals oriented parallel to the sample surface.

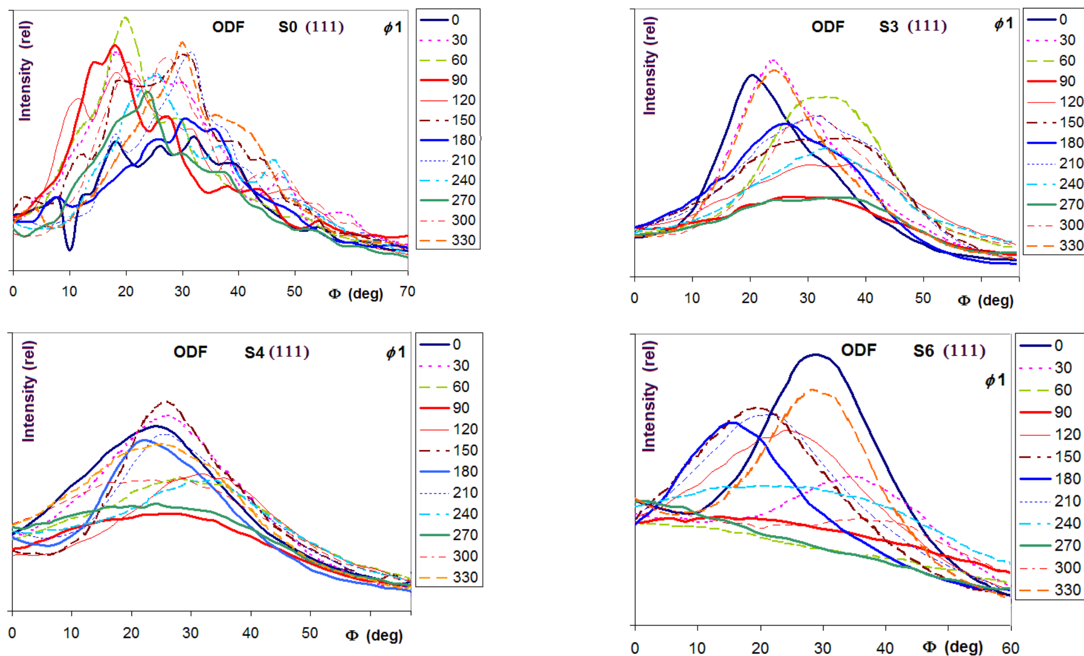

Fig.18 *Fragments of orientation distribution functions for ϕ_2=0 and for all 4 brass samples*

The initial distribution (S0) on Fig.18 is arranged in range 10 to 45 deg of inclination angle. At increasing of deformation level (samples S3, S4 and S6), it is possible to see separation of diffraction intensity peak to Φ angles around 35 and 15 deg. This effect is most noticeable on the sample with the greatest deformation level (S6). Diffraction response depends on the angle of rotation ϕ_1, where we can see a change of the diffraction intensity. Diffraction intensity maxima are identical to the rolling direction of the samples (ϕ_1 = 0 deg). The peaks of intensity are smaller in the perpendicular direction (90 and 270 deg). Detailed analysis of changes in ODF under the influence of mechanical deformation can be done from graphs shown in Fig.19. On this figure, there are visible changes in ODF depending on the angle of rotation $\phi_1 \in (0, 360)$ deg. The effect of changes in

the texture due to mechanical deformation can be monitored through the evaluation of the diffraction intensity peaks shift or also from changes their FWHM.

***Fig.19** The comparison of orientation distribution functions for various angles ϕ_1 at ϕ_2=0 deg. The vertical axis represents the intensity of diffraction response.*

The cumulative chart shown in Fig. 20 was taken from shift of pattern peaks shown in graphs on Fig. 19. The first graph (Fig. 20) shows the response of the diffraction peaks positions depending on the angle of rotation ϕ_1 and second graph shows the dependence of these peaks on the deformation level (ε) of the sample. The graph on the right confirms that the preferred directions are ϕ_1 = 0 deg and ϕ_1 = 180 deg.

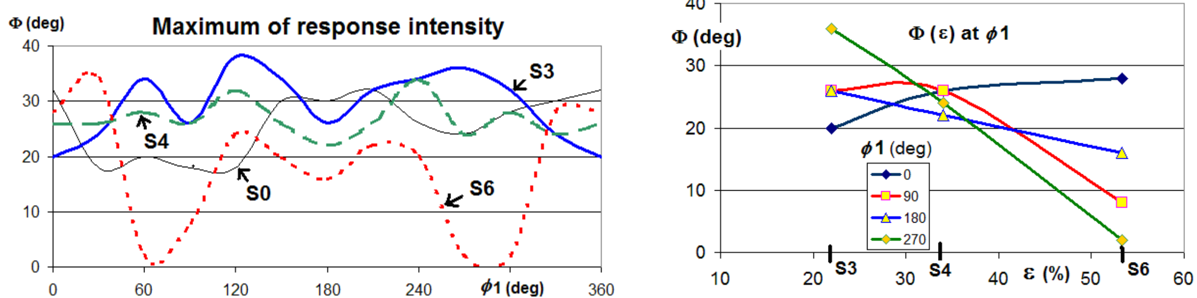

***Fig.20** Picks of diffraction intensity in angle of sample tilt (Φ) in dependence on rotation angle ϕ_1 (left) and deformation level ε (right)*

As an attempt to further evaluation the FWHM method has been done. Waveforms of FWHM derived from ODF curves are shown in Fig. 21: the image on the left shows the dependence of FWHM on the angle of rotation ϕ_1 for various levels of deformation, and the right graph is the dependence of FWHM on the deformation level. As it is shown in that two images the preferred directions are $\phi_1 = 0$ and $\phi_1 = 180$ deg and the minimum values of FWHM are in positions where they are expected.

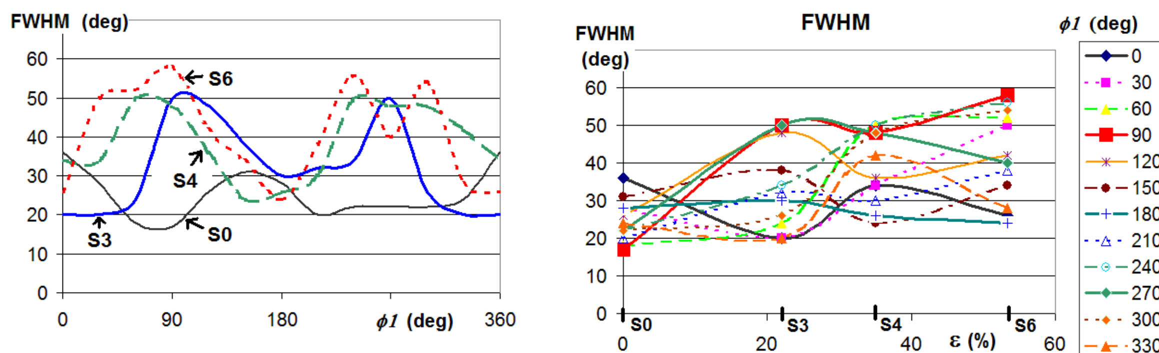

Fig. 21 *FWHM of diffraction intensity in dependence on rotation angle ϕ_1 (left) and deformation level ε (right)*

4 Conclusion

The aim of this study was to show the possibilities of using X-ray diffraction for materials research in particular with regard to changes in the texture of the material during mechanical deformation. Article does not describe all the possibilities of the methodology, so that more detailed information is to be found in the literature, which is enough on this subject (see eg. [13-15]).

Acknowledgements

This work was supported within the project "Trenčín wants to offer high quality and modern education" ITMS no. 26110230099 based on the Operational Programme Education and funded from the European Social Fund.

The authors thank to Assoc. Prof. RNDr. Edmund Dobročka, PhD. from Institute of Electrical engineering SAS Bratislava for measuring of pole figures and his helpful consultations.

References

[1] B. E. Warren: X-Ray Diffraction, Adison-Wesley Publishing Company, Reading, 1969.

[2] K. Birkholz: Thin Film Analysis by X-Ray Scattering, Wiley-VCH, Weinheim, 2006.

[3] Keigo Nagao, Erina Kagami: X-Ray thin film measurement techniques, VII. Pole figure measurement, The Rigaku Journal 27(2), 2011, pp. 6-14.

[4] V. Valvoda, M. Polcarová, P. Lukáč: Basics of structural analysis (*Základy strukturní analýzy)*, Praha, 1992.

[5] D. Firrao, P. Matteis, C. Pozzi, et al.: Microstructural modifications in α-brass targets after small charge explosions, CALPHAD: Computer Coupling of Phase Diagrams and Thermochemistry 33, 2009, p. 76-81.

[6] Tokimasa Go, Takashi Kondoh, Hajime Hirose and Toshihiko Sasaki: Complete Pole Figure Measurement Using only Backreflection Method with Imaging Plate and Application to Three-dimensional Analysis of Texture, JCPDS International Centre for Diffraction Data 2001, Advances in X-ray Analysis, Vol. 44, p. 272-277.

[7] E. Dobročka: Analysis of thin crystallic layers by X-ray diffraction (Analýza kryštalických tenkých vrstiev pomocou difrakcie röntgenového žiarenia), on line in: http://www.matnet.sav.sk/index.php?ID=448 [3.11.2015].

[8] De-Chang Tsai, Weng-Sing Hwang: A Three Dimensional Cellular Automaton Model for the Prediction of Solidification, Materials Transactions, The Japan Institute of Metals, Vol. 52, No. 4 (2011), p. 787 to 794.

[9] V.A. Lubarda: On the effective lattice parameter of binary alloys, Mechanics of Materials 35, 2003, p. 53–68.

[10] T. Bohlke, G. Risy, A. Bertram: A texture component model for anisotropic polycrystal plasticity, Computational Materials Science 32, 2005, p. 284–293.

[11] T. Bohlke, Utz-Uwe Haus b, V. Schulze: Crystallographic texture approximation by quadratic programming, Acta Materialia 54, 2006, p. 1359–1368.

[12] *E. Hujová, V. Áč:* Texture analysis of metal alloys using x-ray diffraction, Conf. Proc. TRANSFER. 2015, the 16th International Scientific Conference, TnUAD Trenčín, ISBN 978-80-8075-6, EAN 9788080757236, p.5.

[13] F. J. Garcia de Abajo c, M.A. Van Hove d, P. Aebi: X-ray photoelectron diffraction study of Cu(111): Multiple scattering investigation, Surface Science 600, 2006, p. 380–385.

[14] N. Jia, F. Roters, P. Eisenlohr, C. Kords, D. Raabe: Non-crystallographic shear banding in crystal plasticity FEM simulations: Example of texture evolution in a-brass, Acta Materialia 60, 2012, p. 1099–1115.

[15] A. K.Verna, A.Singweker, N. Nichichlani, V.Singh, P. Mukhopadhyay: Deformation characterization of cartridge brass, Indian Journal of Engineering & Material Sciences, Vol. 2, August 2013, p. 283-288.